Hindawi
Advances in Mathematical Physics
Volume 2024, Article ID 9306915, 13 pages
https://doi.org/10.1155/2024/9306915

Research Article

Application of Constant Proportional Caputo Fractional Derivative to Thermodiffusion Flow of MHD Radiative Maxwell Fluid under Slip Effect over a Moving Flat Surface with Heat and Mass Diffusion

Adnan Ahmad,[1] M. Nazar ,[1] M. Ahmad ,[1,2] Sayed M. Eldin,[3] Zaib Un Nisa ,[2] Hassan Waqas ,[4] and M. Imran [5]

[1] *Centre for Advanced Studies in Pure and Applied Mathematics, Bahauddin Zakariya University, Multan, Pakistan*
[2] *Department of Mathematics and Statistics, Institute of Southern Punjab, Multan, Pakistan*
[3] *Center of Research, Faculty of Engineering, Future University in Egypt, New Cairo 11835, Egypt*
[4] *School of Energy and Power Engineering, Jiangsu University, Zhenjiang 212013, China*
[5] *Department of Mathematics, Government College University, Faisalabad, Pakistan*

Correspondence should be addressed to Hassan Waqas; syedhasanwaqas@hotmail.com and M. Imran; drmimranchaudhry@gcuf.edu.pk

Received 20 October 2022; Revised 23 July 2023; Accepted 31 July 2023; Published 22 January 2024

Academic Editor: Mohammad W. Alomari

Thermal diffusion is a phenomenon where the concentration gradient or diffusive flux is created due to the temperature gradient. Thermal diffusion is induced because of the higher temperature and uneven distribution of the mixture. Formally, thermal diffusion is called the Soret effect, and it is a crucial factor in a number of natural occurrences like the separation of isotopes technique of purification. In this research paper, Maxwell fluid's flow in the vicinage of a flat plate is discussed by considering the effect of the thermodiffusion subject to the first-order slip at the boundary with the application of a constant proportional Caputo (CPC) fractional derivative. The effect of heat generation and radiation is also taken into consideration, as well as the effect of a magnetic field of constant magnitude. The generalized heat and mass fluxes are considered, and this generalization of heat and mass fluxes is done by utilizing the CPC fractional derivative. After converting the current model's governing equations into a dimensionless form, the temperature, concentration, and velocity fields' analytical solutions are found. By drawing graphs of the temperature, concentration, and velocity fields for the parametric modifications, the results are graphically illustrated. It becomes clear from the results discussion that the outcomes produced by the constant proportional derivative are more decaying than those obtained with the classical differential operator of order one.

1. Introduction

Thermodiffusion is a physical phenomenon that occurs in the mixture of different moving particles with an adverse response to the temperature gradient. In this phenomenon, the particles of smaller inertia tend to move in the region of higher temperature, while the particles with the greater inertia try to move in the area of lower temperature. Formally, this phenomenon is called the Soret effect and has many industrial and biological applications like isotope separation [1, 2].

Slippage of the flowing fluid over a flat surface is important in many complex flows of non-Newtonian fluids. Slip of the fluid occurs at the boundary when there is relative motion between fluid and boundary. This mechanical situation is addressed properly by the Robin-type boundary condition and specifically, it is known as the slip boundary condition. The slip effect is formulated by many theorists to address the different geometric situations for the boundary layer flows. Vieru et al. [3] explained the aspect of slip for second-grade fluid flow. Tahir et al. [4] considered Maxwell fluid motion over an oscillation surface. Jameel and Khan [5] discussed an impulsive flow over the flat plate. Hayat et al. [6] studied the Stokes flow for the slip condition. Imran et al. [7] applied the first order slip for the motion of the non-Newtonian fluid. Sajid et al. [8] explained the slippage motion of the rate-type fluid. Hayat et al. [9] studied the flow of Maxwell fluid between the plates under the influence of MHD and radiation. Ramesh et al. [10] studied the Maxwell fluid over a stretching sheet and discussed the impact of radiation on the motion of the fluid. Khan et al. [11] reported the flow of Maxwell fluid by taking into account the influence of radiation. Chen et al. [12] utilized the fractional derivatives boundary layer flow of Maxwell fluid on an unsteady stretching surface and obtained the results for the velocity. Over a vertical plate, Imran et al. [13] considered a slippage flow of a radiative fluid.

Opangua et al. [14] explained the effect of slip on the flow of coupled stressed fluid. Hayat and Asghar [15] and Hayat et al. [16, 17] considered the impact of heat transfer over the slippage flow of peristaltic fluid. Shakeel et al. [18] employed the slip effect to rate-type fluid over an accelerating plate. Shah et al. [19] applied the fractional calculus to get the generalized results for the unidirectional velocity for Maxwell fluid. Shah et al. [20] used the slip conditions at the boundary for MHD Carreau fluid through a porous regime. Freidoonimehr and Jafari [21] also employed slip conditions at the boundary for MHD nanofluid flow. Schneider [22] considered the motion of electrorheological suspensions and laid out the impact of wall slip on the rheological behavior of the suspension. Raza [23] stagnation point flow of Casson fluid by considering the impact of slip. Norouzi et al. [24] investigated the flow of Oldroyd-B fluid in the cylindrical domain by studying the effect of slip at the boundary. Fetecau et al. [25] discussed the flow of Newtonian fluid by taking into account the effect of slip at the edge of the flow. Khan et al. [26] applied the slip attribute to the viscous nanofluid flow and obtained the velocity field.

Khan et al. [27] discussed the impact of the transfer of heat on the flow of Maxwell fluid. Chu et al. [28] studied nanofluid flow with four different types of nanoparticles, which are subject to the nonhomogenous source of heat, and applied the numerical technique to obtain the approximated solutions. Alqahtani et al. [29] did a detailed analysis of the impact of radiation on the flow of nanofluid. Puneeth et al. [30] explained the effect of convection on nanofluid's flow over a sheet. Alharbi et al. [31] illustrated the effect of the bioconvective hydromagnetic flow of Oldroyd-B nanofluid over a stretching surface having pores. Khan et al. [32] took under consideration the unsteady flow of hybrid nanofluid on a radiated porous surface subject to the magnetic field. Qaiser et al. [33] investigated the effects of active energy and entropy for nanofluid flow subject to viscous dissipation and cross-diffusion. Some other investigations related to nanofluid flow in different physical situations have been done [33–39].

The Maxwell fluid model is suitable for momentum, heat, and mass transfer phenomena as it captures relaxation time effects. Khan et al. [40] discussed the generalized conclusions for the flow of Maxwell fluid by taking into consideration the modified Fick's and Fourier laws for mass and heat transfer, respectively. Khan et al. [41] utilized the Cattaneo–Christov mechanism for the heat transfer of Maxwell fluid through a closed path. Tang et al. [42] discussed the flow of Maxwell fluid subject to uniform heat flux and thermal radiation by applying the fractional derivative. Mansoor et al. [43] also considered the Maxwell fluid's flow, and the effect of chemical reaction over the velocity field is explained.

The fractional derivatives are flexible and nonlocal because the order of the fractional derivatives can be any real number. Due to nonlocality and flexibility, the fractional derivatives are suitable for approximating real data values with more reliability than classical derivatives for the effect of global interactions (nonlocality of space) and memory (nonlocality of time). Nowadays, fractional calculus is applied efficiently to explain the complex flow phenomenon. There are different approaches to the fractional derivative used by mathematicians [44–47], and a recent development in the fractional is the constant proportional Caputo (CPC) derivative proposed by Baleanu et al. [48].

The thermodiffusion, formally known as the Soret effect, occurs when a concentration gradient is generated due to a temperature gradient. This effect is significant for complex mixtures containing different species of diverse sizes and polarities, for example, in the petroleum system. The principal interest of this article is to widen the research work done in [25] by taking the flow of Maxwell fluid, and the flow modeling is done with a fractional derivative of the recent approach, namely the constant Caputo fractional derivative. The graphical illustration of field variables is done by using MATHCAD software. In addition to this, the slip at the boundary is analyzed with other parameters. Such work addressing the thermodiffusion effect for Maxwell fluid's flow with CPC fractional derivative is yet to be reported in the literature.

2. Mathematical Description

Considered Maxwell fluid flowing over a vertical plate. The vertical plate is situated in the xz-plane in a way that the y-axis becomes normal to the place of the plate, as indicated in Figure 1. At first, the plate with the fluid is not moving; after the time $t > 0$, the plate starts moving with the velocity $V_0 f(t)$, and by considering the slip effect over the plate fluid also move. Under the assumption, the Maxwell fluid flow model in mathematical form is as follows [25, 27]:

$$\begin{aligned}\rho\left(\lambda_1\frac{\partial}{\partial t}+1\right)\frac{\partial u}{\partial t}=\mu\frac{\partial^2 u}{\partial y^2}+g(\rho\beta_T)\left(1+\lambda_1\frac{\partial}{\partial t}\right)[T-T_\infty]\\+g(\rho\beta_C)\left(1+\lambda_1\frac{\partial}{\partial t}\right)[C-C_\infty]-\left(1+\lambda_1\frac{\partial}{\partial t}\right)B_0^2\sigma u,\end{aligned} \tag{1}$$

$$k\frac{\partial^2 T}{\partial y^2}-\frac{\partial q_r}{\partial y}-Q_0[T-T_\infty]-(\rho c_p)\frac{\partial T}{\partial t}=0, \tag{2}$$

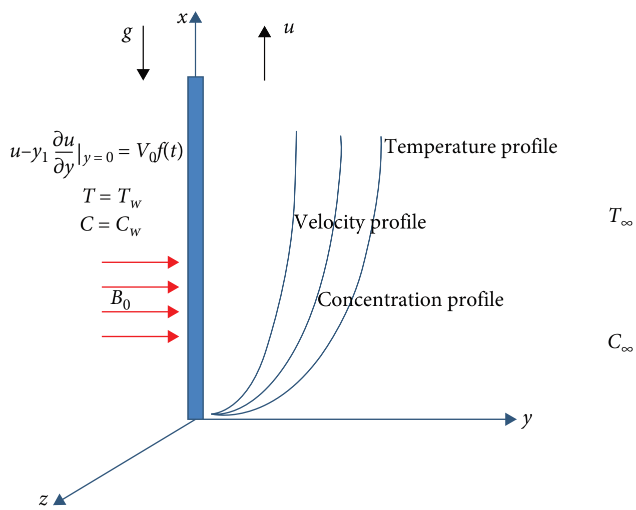

Figure 1: Flow geometry.

$$D_m \frac{\partial^2 C}{\partial y^2} + \frac{D_m k_T}{T_m} \frac{\partial^2 T}{\partial y^2} - \frac{\partial C}{\partial t} = 0, \tag{3}$$

and related conditions

$$\text{for } t = 0 \Rightarrow u = 0, T = T_\infty, \quad C = C_\infty, \tag{4}$$

$$u - \gamma_1 \frac{\partial u}{\partial y}\Big|_{y=0} = V_0 f(t), \quad T = T_w, \quad C = C_w, \quad y = 0, \tag{5}$$

$$u \to 0, T \to T_\infty, \quad C \to C_\infty, \quad y \to \infty. \tag{6}$$

The radiated flux from Equation (2) is approximated by using the Roseland approach [49, 50] for the minor temperature difference between the temperature of the fluid and the free stream temperature [51, 52].

$$k[N_r + 1]\left(\frac{\partial^2}{\partial y^2} - (\rho c_p)\frac{\partial}{\partial t}\right) T(y,t) = Q_0[T(y,t) - T_\infty], \tag{7}$$

where $N_r = \frac{16\sigma_1 T_\infty^3}{3kk_1}$ is the radiation parameter.

Nondimensional relations [25]

$$\begin{aligned} &u^* = \frac{u}{V_0}, \quad y^* = \frac{yV_0}{\nu}, \quad t^* = \frac{V_0^2}{\nu}t, \quad C^* = \frac{C - C_\infty}{C_w - C_\infty}, \quad T^* = \frac{T - T_\infty}{T_w - T_\infty}, \\ &Q^* = \frac{\nu Q_0}{(\rho c_p)V_0^2}, \quad \gamma_1^* = \frac{V_0}{\nu}\gamma_1, \quad f^*(t^*) = f\left(\frac{\nu}{V_0^2}t^*\right), \quad \lambda = \frac{V_0^2}{\nu}\lambda_1, \end{aligned} \tag{8}$$

with $V_0 = [\nu g \beta_T (T_w - T_\infty)]^{1/3}$ is specific velocity, and after using Equations (1)–(7) and Equation (8) dimensionless model takes the following form:

$$\left(\lambda \frac{\partial}{\partial t} + 1\right)\frac{\partial u}{\partial t} = \frac{\partial^2 u}{\partial y^2} + \left(1 + \lambda \frac{\partial}{\partial t}\right)[T - Mu + NC], \tag{9}$$

$$\frac{\partial T}{\partial t} = \frac{1}{\mathrm{Pr_{eff}}}\frac{\partial^2 T}{\partial y^2} - QT, \tag{10}$$

$$\mathrm{ScSr}\frac{\partial^2 T}{\partial y^2} = \mathrm{Sc}\frac{\partial C}{\partial t} - \frac{\partial^2 C}{\partial y^2}, \tag{11}$$

and corresponding dimensionless initial conditions and boundary conditions

$$u = 0, T = 0, C = 0, t = 0, \tag{12}$$

$$f(t) = u - \gamma_1 \tfrac{\partial u}{\partial y}\big|_{y=0}, \quad T = 1, C = 1, y = 0, \tag{13}$$

$$u \to 0, T \to 0, C \to 0, y \to \infty, \tag{14}$$

$$\begin{aligned} &N = \frac{\rho\beta_C[C_w - C_\infty]}{\rho\beta_T[T_w - T_\infty]}, \quad \mathrm{Pr_{eff}} = \frac{\mathrm{Pr}}{Nr + 1}, \quad M = \frac{\nu\sigma B_0^2}{\rho V_0^2}, \\ &\mathrm{Sc} = \frac{\nu}{D_m}, \quad \mathrm{Sr} = \frac{D_m k_T [T_w - T_\infty]}{\nu T_m [C_w - C_\infty]}, Q = \frac{\nu Q_0}{\rho c_p V_0^2}, \end{aligned} \tag{15}$$

where N is the ratio of the thermal Grashof number to the mass Grashof number, $\mathrm{Pr_{eff}}$ effective Prandtl number, M is a nondimensional magnetic parameter, Sc is the Schmidt number, Q is the nondimensional heat generation parameter, and Sr is the Soret effect parameter.

3. Classical Solution of the Model

3.1. Temperature. Equation (10) is reduced to an ordinary differential equation as follows:

$$Pr_{\mathrm{eff}} q\overline{T}(y,q) + Q\overline{T}(y,q) = \frac{\partial^2 \overline{T}(y,q)}{\partial y^2}. \tag{16}$$

Equation (16) is solved by conditions given below:

$$T(\infty, q) = 0, \overline{T}(0,q) = q^{-1}, \tag{17}$$

and solution transformed for temperature is as follows:

$$\overline{T}(y,q) = \frac{1}{q} e^{\left[-y\sqrt{Pr_{\mathrm{eff}}}\sqrt{Q+q}\right]}. \tag{18}$$

3.2. Concentration. Equation (11), by using the Laplace transform, is reduced to an ODE as follows:

$$\mathrm{Sc}q\overline{C}(y,q)=\frac{\partial^2\overline{C}(y,q)}{\partial y^2}+\mathrm{Sr}\frac{\partial^2\overline{T}(y,q)}{\partial y^2}. \tag{19}$$

Equation (19) is solved by the conditions as follows:

$$C(\infty,q)=0,\overline{C}(0,q)=q^{-1}. \tag{20}$$

The solutions are given below:

$$\begin{aligned}\overline{C}(y,q)&=\frac{1}{q}\exp\left(-y\sqrt{\mathrm{Sc}q}\right)\\&+\frac{\mathrm{ScSrPr_{eff}}(Q+q)}{[(Pr_{\mathrm{eff}}-\mathrm{Sc})q+Q\,Pr_{\mathrm{eff}}]q}\exp\left[-y\sqrt{\mathrm{Sc}q}\right].\\&-\frac{\mathrm{ScSrPr_{eff}}(Q+q)\exp\left[-y\sqrt{Pr_{\mathrm{eff}}(Q+q)}\right]}{q[q(Pr_{\mathrm{eff}}-\mathrm{Sc})+Pr_{\mathrm{eff}}Q]}\end{aligned} \tag{21}$$

3.3. Velocity Field. Equation (9), by using the Laplace transform, is reduced to the following:

$$\begin{aligned}&\left[1+\lambda\left(\frac{k_1(\alpha)}{q}+k_0(\alpha)\right)q^\alpha\right]q\overline{u}(y,q)=\frac{\partial^2\overline{u}(y,q)}{\partial y^2}\\&+\left[1+\lambda\left(\frac{k_1(\alpha)}{q}+k_0(\alpha)\right)q^\alpha\right]\\&\times\left[\overline{T}(q,y)-M\overline{u}(q,y)+N\overline{C}(q,y)\right].\end{aligned} \tag{22}$$

Equation (22) is solved by the following transformed condition:

$$\overline{u}(\infty,q)=0,\overline{u}(0,q)-\gamma\left.\frac{\partial\overline{u}(y,q)}{\partial y}\right|_{y=0}=f(q), \tag{23}$$

and its solution is as follows:

$$\begin{aligned}\overline{u}(y,q)&=\frac{F(q)e^{-y\sqrt{[1+\lambda q][M+q]}}}{1+\gamma_1\sqrt{[1+\lambda q][M+q]}}+\frac{[1+\lambda q]\left[1+\gamma_1\sqrt{Pr_{\mathrm{eff}}(Q+q)}\right]}{[Pr_{\mathrm{eff}}(Q+q)-(M+q)(1+\lambda q)]q}\\&\times\left[1-\frac{N\mathrm{ScSrPr_{eff}}(Q+q)}{[Pr_{\mathrm{eff}}-\mathrm{Sc}]q+Q\,Pr_{\mathrm{eff}}}\right]\left[\frac{e^{-y\sqrt{[1+\lambda q][M+q]}}}{1+\gamma_1\sqrt{[1+\lambda q][M+q]}}-\frac{e^{-y\sqrt{Pr_{\mathrm{eff}}(Q+q)}}}{1+\gamma_1\sqrt{Pr_{\mathrm{eff}}[Q+q]}}\right]\\&+\frac{N(\lambda q+1)\left[1+\gamma_1\sqrt{\mathrm{Sc}q}\right]}{[\mathrm{Sc}q-(q+M)[\lambda q+1]]q}\left[1+\frac{\mathrm{ScPr_{eff}Sr}[Q+q]}{q(Pr_{\mathrm{eff}}-\mathrm{Sc})+Q\,Pr_{\mathrm{eff}}}\right]\\&\times\left[\frac{e^{-y\sqrt{[\lambda q+][M+q]}}}{1+\gamma_1\sqrt{[\lambda q+1][M+q]}}-\frac{e^{-y\sqrt{\mathrm{Sc}q}}}{1+\gamma_1\sqrt{\mathrm{Sc}q}}\right].\end{aligned} \tag{24}$$

4. Generalization with CPC

In this section, the flow model is generalized by introducing the generalized constitutive relations for momentum, heat, and mass fluxes. The generalization is made by newly developed fractional derivative, known as CPC fractional derivative denoted by ${}^{\mathrm{CPC}}D_t^\alpha$ and defined as follows [48]:

$${}^{\mathrm{CPC}}D_t^\alpha f(t)=\frac{1}{\Gamma(1-\alpha)}\int_0^t[k_1(\alpha)f(s)+k_0(\alpha)f'(\tau)](t-s)^{-\alpha}ds\,, \tag{25}$$

and its Laplace transform is defined as follows [48]:

$$£\{{}^{\mathrm{CPC}}D_t^\alpha f(t)\}=\left(\frac{k_1(\alpha)}{q}+k_0(\alpha)\right)q^\alpha\overline{f}(q)-k_0(\alpha)q^{\alpha-1}f(0). \tag{26}$$

The momentum equation

$$\left(\lambda\frac{\partial}{\partial t}+1\right)\frac{\partial u}{\partial t}=\frac{\partial\tau_\alpha(y,t)}{\partial y}+\left(\lambda\frac{\partial}{\partial t}+1\right)[T-Mu+NC], \tag{27}$$

where $\tau_\alpha(y,t)$ is the shared stress is given by the following generalized constitutive relation

$$\tau_\alpha(y,t)={}^{\mathrm{CPC}}D_t^\alpha\frac{\partial u(y,t)}{\partial y}. \tag{28}$$

The equation for the temperature profile in generalized form is as follows:

$$Pr_{\mathrm{eff}}\frac{\partial T(y,t)}{\partial t}=-\frac{\partial q_\beta(y,t)}{\partial y}-Pr_{\mathrm{eff}}QT(y,t), \tag{29}$$

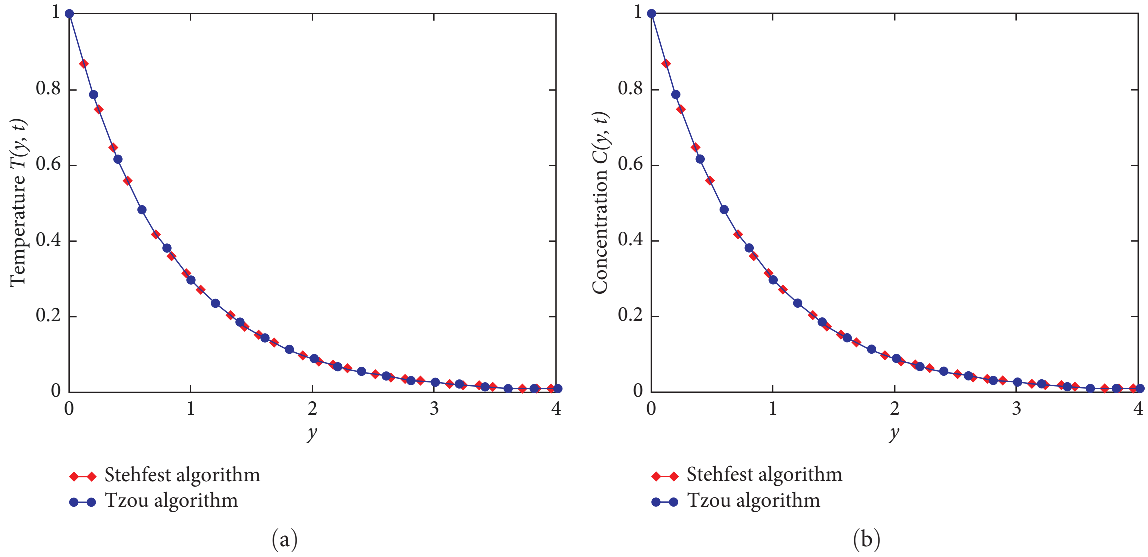

FIGURE 2: Inverse of temperature (a) and concentration (b) fields.

and $q_\beta(y,t)$ is given in the equation below:

$$q_\beta(y,t) = -{}^{\mathrm{CPC}}D_t^\beta \frac{\partial T(y,t)}{\partial y}. \tag{30}$$

The diffusion balance in terms of generalized mass flux is as follows:

$$\mathrm{Sc}\frac{\partial C(y,t)}{\partial t} = -\frac{\partial q_\gamma(y,t)}{\partial y} + \mathrm{ScSr}\frac{\partial^2 T(y,t)}{\partial y^2}, \tag{31}$$

where the generalized mass flux is as follows:

$$q_\gamma(y,t) = -{}^{\mathrm{CPC}}D_t^\gamma \frac{\partial C(y,t)}{\partial y}. \tag{32}$$

Using the generalized constitutive relations for stress, heat flux, and mass flux from Equations (28), (30), and (32) into Equations (27), (29), and (31), respectively

$$\left(\lambda\frac{\partial}{\partial t}+1\right)\frac{\partial u}{\partial t} = \frac{\partial\left[{}^{\mathrm{CPC}}D_t^\alpha \frac{\partial u(y,t)}{\partial y}\right]}{\partial y} + \left(\lambda\frac{\partial}{\partial t}+1\right)[T(y,t) - Mu(y,t) + NC(y,t)], \tag{33}$$

$$\frac{\partial T(y,t)}{\partial t} = -\frac{1}{Pr_{\mathrm{eff}}}\frac{\partial\left[-{}^{\mathrm{CPC}}D_t^\beta \frac{\partial T(y,t)}{\partial y}\right]}{\partial y} - QT(y,t), \tag{34}$$

and

$$\mathrm{Sc}\frac{\partial C}{\partial t} = -\frac{\partial\left[-{}^{\mathrm{CPC}}D_t^\gamma \frac{\partial C(y,t)}{\partial y}\right]}{\partial y} + \mathrm{ScSr}\frac{\partial^2 T}{\partial y^2}. \tag{35}$$

5. Generalized Solution to the Problem

5.1. Generalized Temperature Field. Equation (34) is transformed as below:

$$q\overline{T}(y,q) = \frac{1}{Pr_{\mathrm{eff}}}\left(\frac{k_1(\beta)}{q}+k_0(\beta)\right)q^\beta \frac{\partial^2 \overline{T}(y,q)}{\partial y^2} - Q\overline{T}(y,q), \quad y>0. \tag{36}$$

Equation (36) is solved under the conditions in Equation (17) is as follows:

$$\overline{T}(y,q) = \frac{1}{q}\exp\left[-y\sqrt{\frac{Pr_{\mathrm{eff}}\,q^{1-\beta}(q+Q)}{[k_1(\beta)+k_0(\beta)q]}}\right]. \tag{37}$$

In Equation (37), the expressions under the root are complicated, and it is not an easy task to invert the Laplace transform. Therefore, the inversion of the Laplace is obtained by executing Stehfest's algorithm [53] and Tzou's [54], and the outcomes of the algorithms are presented in Figure 2(a).

5.2. Generalized Concentration Field. From Equation (35)

$$\mathrm{Sc}q\overline{C}(y,q)=\left(\frac{k_1(\gamma)}{q}+k_0(\gamma)\right)q^{\gamma}\frac{\partial^2\overline{C}(y,q)}{\partial y^2}+\mathrm{ScSr}\frac{\partial^2\overline{T}(y,q)}{\partial y^2},\quad y>0. \tag{38}$$

Equation (38) is solved under the transformed boundary conditions in Equation (20) as follows:

$$\begin{aligned}\overline{C}(y,q)=&\frac{1}{q}\exp\left[-y\sqrt{\frac{\mathrm{Sc}q^{2-\gamma}}{[k_1(\gamma)+k_0(\gamma)q]}}\right]\\&+\frac{\mathrm{ScSrPr_{eff}}(Q+q)q^{1-\gamma}}{[(Pr_{\mathrm{eff}}-\mathrm{Sc})q+QPr_{\mathrm{eff}}][k_1(\gamma)+k_0(\gamma)q]q}\exp\left[-y\sqrt{\frac{\mathrm{Sc}q^{2-\gamma}}{[k_1(\gamma)+k_0(\gamma)q]}}\right]\\&-\frac{\mathrm{ScSrPr_{eff}}(Q+q)q^{1-\gamma}}{[(Pr_{\mathrm{eff}}-\mathrm{Sc})q+QPr_{\mathrm{eff}}][k_1(\gamma)+k_0(\gamma)q]q}\exp\left[-y\sqrt{\frac{Pr_{\mathrm{eff}}q^{1-\gamma}(q+Q)}{[k_1(\gamma)+k_0(\gamma)q]}}\right].\end{aligned} \tag{39}$$

Equation (39) is inverted by algorithms and shown in Figure 2(b) [53, 54].

5.3. Generalized Velocity Field. Equation (33) is reduced to an ODE by using Laplace transform as follows:

$$(1+\lambda q)q\overline{u}=\left(\frac{k_1(\alpha)}{q}+k_0(\alpha)\right)q^{\alpha}\frac{\partial^2\overline{u}}{\partial y^2}+[\lambda q+1]\left[\overline{T}-M\overline{u}+N\overline{C}\right], \tag{40}$$

$$\begin{aligned}&\frac{\partial^2\overline{u}(y,q)}{\partial y^2}-\frac{(1+\lambda q)(q^{2-\alpha}+M)}{[k_1(\alpha)+k_0(\alpha)q]}\overline{u}(y,q)\\&=-\frac{(1+\lambda q)q^{1-\alpha}}{[k_1(\alpha)+k_0(\alpha)q]}\left[\overline{T}(y,t)+N\overline{C}(y,q)(y,q)\right].\end{aligned} \tag{41}$$

Equation (41) is solved subject to the condition in Equation (23) as follows:

$$\begin{aligned}\overline{u}(y,q)=&\frac{F(q)\exp\left[-y\sqrt{\frac{[\lambda q+1](q^{2-\alpha}+M)}{[k_1(\alpha)+k_0(\alpha)q]}}\right]}{1+\gamma_1\sqrt{\frac{(1+\lambda q)(q^{2-\alpha}+M)}{[k_1(\alpha)+k_0(\alpha)q]}}}+\frac{(1+\lambda q)\left(1+\gamma_1\sqrt{\frac{Pr_{\mathrm{eff}}q^{1-\beta}(q+Q)}{[k_1(\beta)+k_0(\beta)q]}}\right)}{[(q+Q)Pr_{\mathrm{eff}}-(M+q^{2-\beta})(1+\lambda q)]q}\\&\times\left[1-\frac{N\mathrm{ScSrPr_{eff}}(Q+q)q^{-\beta}}{[(Pr_{\mathrm{eff}}-Sc)q+QPr_{\mathrm{eff}}][k_1(\beta)+k_0(\beta)q]}\right]\\&\times\left[\frac{\exp\left(-y\sqrt{\frac{(1+\lambda q)(q^{2-\alpha}+M)}{[k_1(\alpha)+k_0(\alpha)q]}}\right)}{1+\gamma_1\sqrt{\frac{(1+\lambda q)(q^{2-\alpha}+M)}{[k_1(\alpha)+k_0(\alpha)q]}}}-\frac{\exp\left(-y\sqrt{\frac{Pr_{\mathrm{eff}}q^{1-\beta}(q+Q)}{[k_1(\beta)+k_0(\beta)q]}}\right)}{1+\gamma_1\sqrt{\frac{Pr_{\mathrm{eff}}q^{1-\beta}(q+Q)}{[k_1(\beta)+k_0(\beta)q]}}}\right]\\&+\frac{N[\lambda q+1]\left[1+\gamma_1\sqrt{\frac{\mathrm{Sc}q^{2-\alpha}}{[k_1(\alpha)+k_0(\alpha)q]}}\right]}{q[\mathrm{Sc}q-(q+M)(\lambda q+)]}\left[1+\frac{\mathrm{ScPr_{eff}Sr}(Q+q)q^{-\gamma}}{[q[Pr_{\mathrm{eff}}-\mathrm{Sc}]+QPr_{\mathrm{eff}}][k_1(\gamma)+k_0(\gamma)q]}\right]\\&\times\left[\frac{\exp\left(-y\sqrt{\frac{(1+\lambda q)(q^{2-\alpha}+M)}{[k_1(\alpha)+k_0(\alpha)q]}}\right)}{1+\gamma_1\sqrt{\frac{[\lambda q+1](q^{2-\alpha}+M)}{[k_1(\alpha)+k_0(\alpha)q]}}}-\frac{\exp\left(-y\sqrt{\frac{\mathrm{Sc}q^{2-\gamma}}{[k_1(\gamma)+k_0(\gamma)q]}}\right)}{1+\gamma_1\sqrt{\frac{\mathrm{Sc}q^{2-\gamma}}{[k_1(\gamma)+k_0(\gamma)q]}}}\right].\end{aligned} \tag{42}$$

Equation (42) in its present form cannot invert in the domain, so its inverse is obtained numerically by the suitable algorithm known as Stehfest's algorithm [53] and Tzou's [54], and the outcomes of this process are presented in and presented in Figures 3(a) and 3(b) for no-slip condition and slip conditions.

6. Results and Discussion

The motion of Maxwell fluid on a flat surface is discussed by considering the effect of the thermodiffusion subject to the first-order slip at the boundary. The effect of heat generation and radiation is also considered with the effect of the

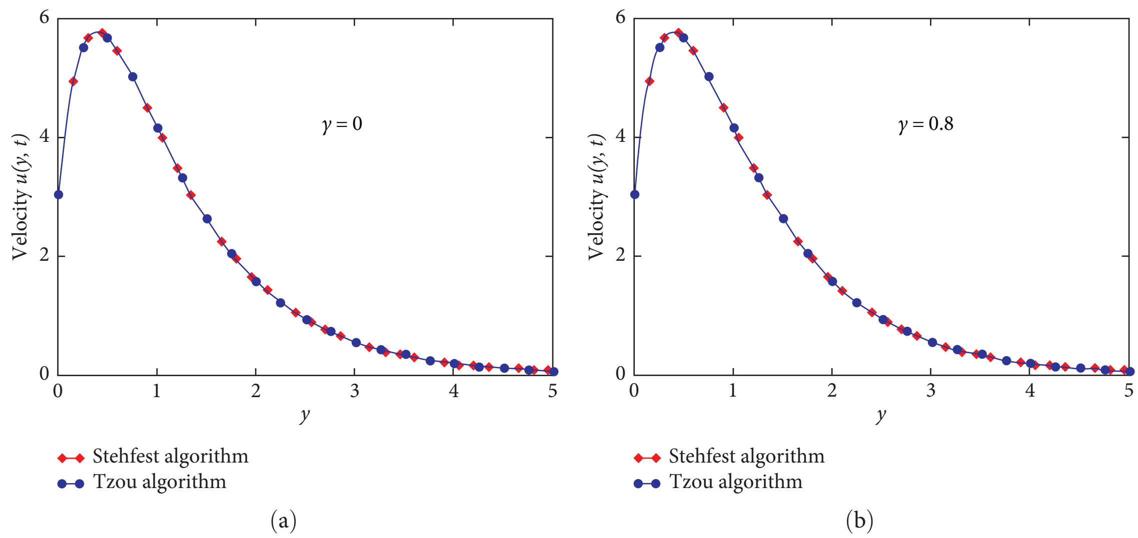

Figure 3: Inverse of the velocity field for (a) for no slip and (b) for slip.

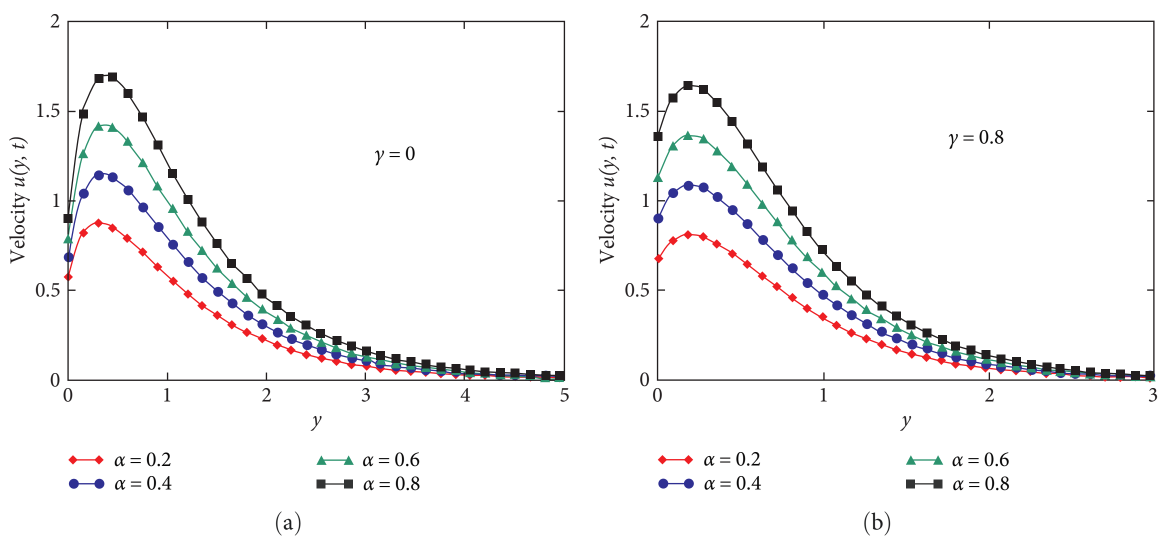

Figure 4: Velocity for variation of α (a) for no slip and (b) for slip $N = 0.5$, $Pr = 1.5$, $\mathrm{Sc} = 0.5$, $\mathrm{Sr} = 1.5$, $M = 0.5$, $\lambda = 2.5$.

magnetic field of constant magnitude. The generalized heat and mass fluxes are considered, and generalization is made by considering the new hybrid fractional derivative. The graphical illustrations for different parametric values are done using the same graphics of velocity against y.

The primary goal of this research is to study the objectivity of the fractional parameter over the velocity field. For this purpose, Figures 4(a) and 4(b) are plotted, and the impact of a fractional parameter over the flow is explained for slip and no slip. The outlines of profiles present an elevating trend for enhancing values of fractional parameters, and this peak in the velocity profiles is seen because of the power law kernel of fractional derivative. In the case of the CPC fractional derivative, the kernel of the operator obeys the power law. Moreover, the subjectivity of velocity for the variation of the other parameter is also explained graphically. The parameter is referred to the relative effect of bouncy forces. Figures 5 and 6 show the effect on the velocity of Maxwell fluid for both positive and negative values. The positive value of N means there is a supporting bouncy for the fluid flow, and the negative value means there is an opposing bouncy to the fluid flow. The results of positive values over fluid velocity is addressed in Figure 7. As $Q > 0$ refers to the heat absorption and more energy in the flow domain due to this fluid motion increases for the growing values of Q as shown in Figure 7. The negative value of Q refers to the heat generation in the flow domain, and some energy is lost due to this fluid velocity decreases, which is revealed in Figure 8.

In Figure 9, the influence of Sc is discussed, and a decreasing trend is seen against the elevating value of Sc because for the elevating value of Sc, momentum diffusivity is dominant; therefore, the velocity field decreases for the increasing values of Sc. The Soret effect Sr over the velocity field is seen in Figure 10, and from the outline of Figure 10, it

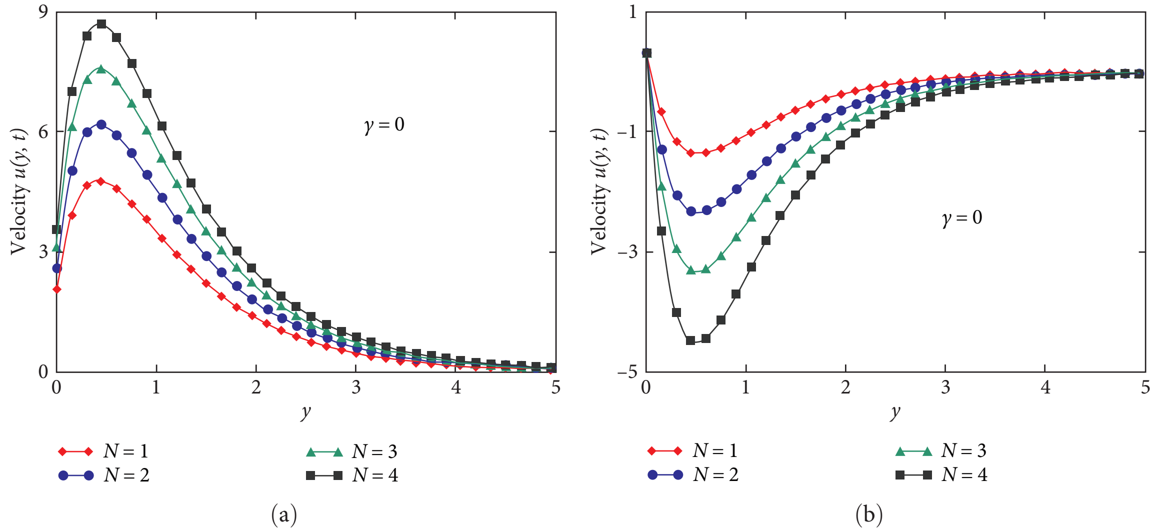

FIGURE 5: Effect of N positive (a) and negative (b) over velocity with no slip $\alpha = 0.5$, $Pr = 1.5$, $\mathrm{Sc} = 0.5$, $\mathrm{Sr} = 1.5$, $M = 0.5$, $\lambda = 2.5$.

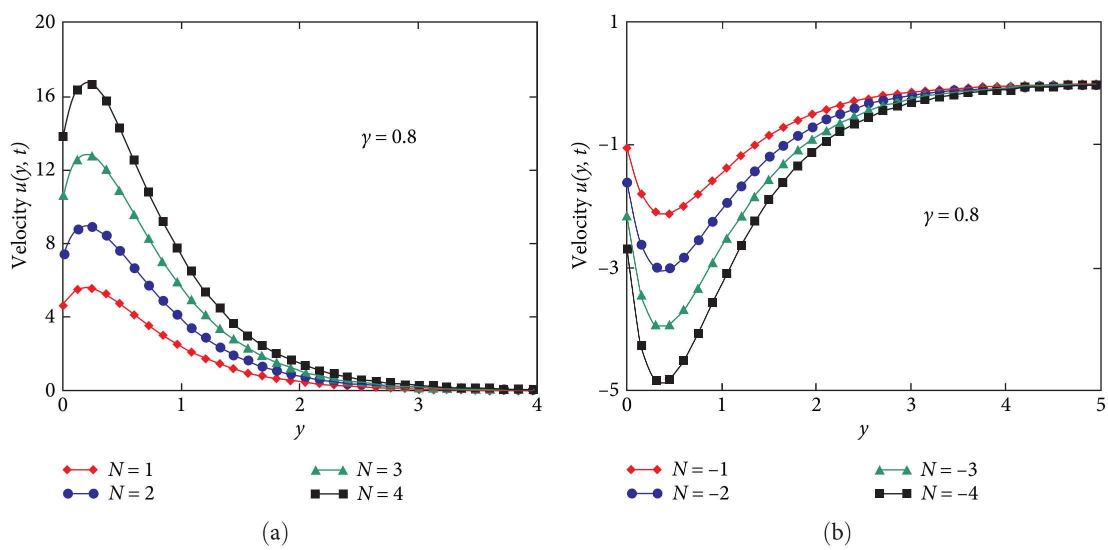

FIGURE 6: Effect of N positive (a) and negative (b) over velocity in the presence of slip, $\alpha = 0.5$, $Pr = 1.5$, $\mathrm{Sc} = 0.5$, $\mathrm{Sr} = 1.5$, $M = 0.5$, $\lambda = 2.5$.

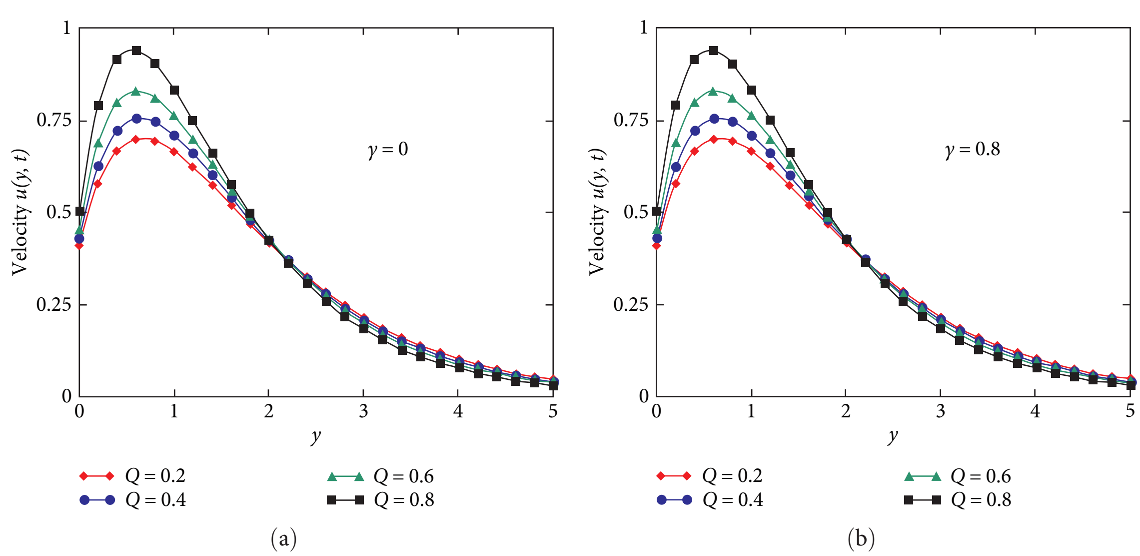

FIGURE 7: Effect of positive Q over velocity (a) for no slip and (b) for slip $\alpha = 0.5$, $Pr = 1.5$, $\mathrm{Sc} = 0.5$, $\mathrm{Sr} = 1.5$, $M = 0.5$, $\lambda = 2.5$.

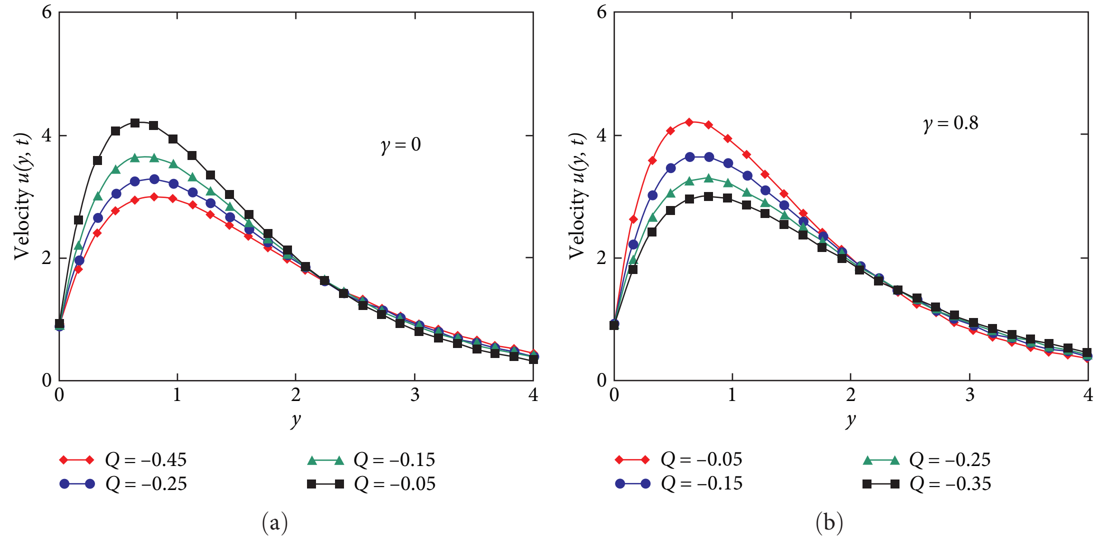

FIGURE 8: Effect of negative Q over velocity (a) for no slip and (b) for slip $\alpha = 0.5$, $Pr = 1.5$, $\mathrm{Sc} = 0.5$, $\mathrm{Sr} = 1.5$, $M = 0.5$, $\lambda = 2.5$.

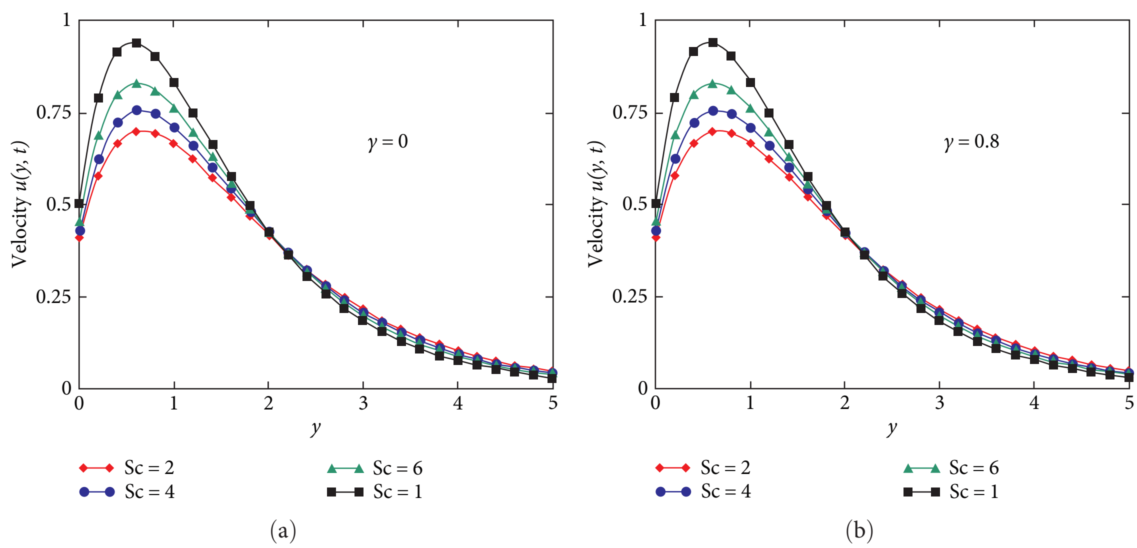

FIGURE 9: Effect of Sc over velocity (a) for no slip and (b) for slip $N = 0.5$, $Pr = 1.5$, $Q = 0.5$, $\mathrm{Sr} = 1.5$, $M = 0.5$, $\lambda = 2.5$, $\alpha = 0.5$.

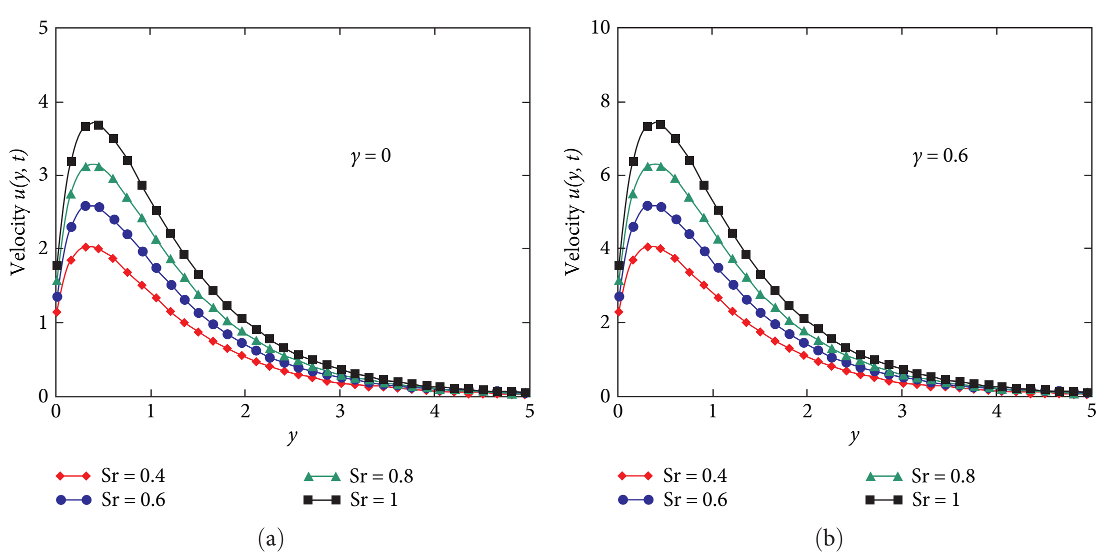

FIGURE 10: Effect of Sr over velocity (a) for no slip and (b) for slip $N = 0.5$, $Pr = 1.5$, $\mathrm{Sc} = 0.5$, $Q = 0.5$, $M = 0.5$, $\lambda = 2.5$, $\alpha = 0.5$.

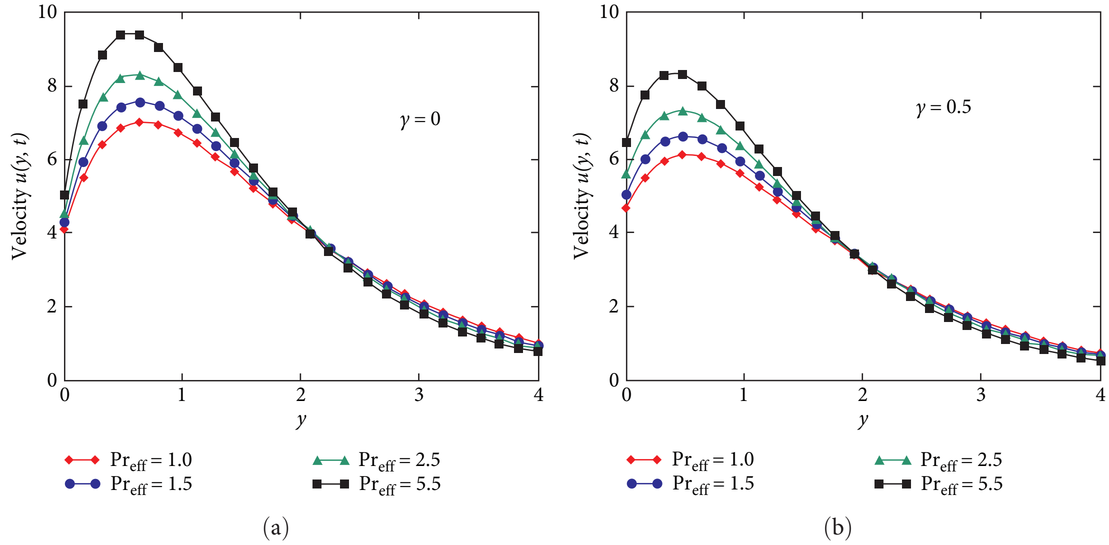

FIGURE 11: Effect of Pr_{eff} over velocity (a) for no slip and (b) for slip $N = 0.5$, $Q = 0.5$, $\mathrm{Sc} = 0.5$, $\mathrm{Sr} = 1.5$, $M = 0.5$, $\lambda = 2.5$, $\alpha = 0.5$.

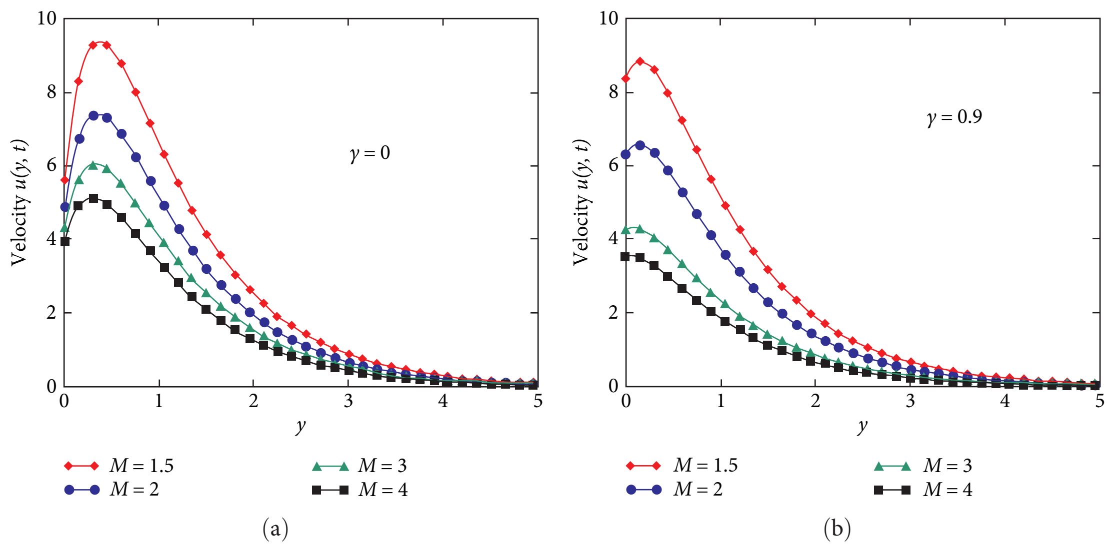

FIGURE 12: Velocity for Sr variation (a) for no slip and (b) for slip $N = 0.5$, $Q = 0.5$, $\mathrm{Sc} = 0.5$, $\mathrm{Sr} = 1.5$, $Pr = 1.5$, $\lambda = 2.5$, $\alpha = 0.5$.

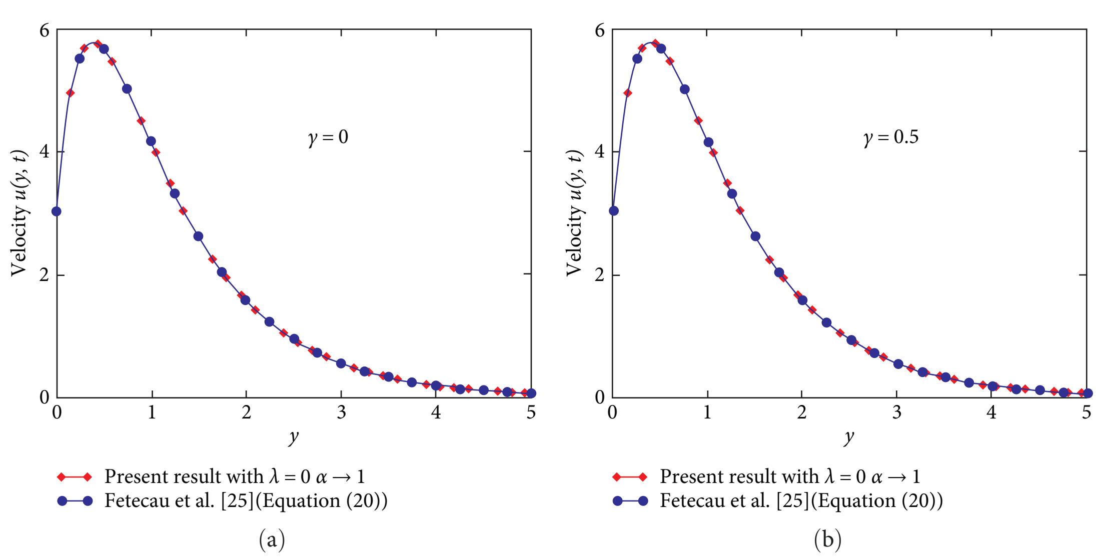

FIGURE 13: Velocity comparison with Fetecau et al. [25] (a) for no slip and (b) for slip $N = 0.5$, $Q = 0.5$, $\mathrm{Sc} = 0.5$, $\mathrm{Sr} = 1.5$, $M = 0.5$, $Pr = 1.5$.

is revealed that elevating Sr accelerates the fluid flow. In Figure 11, the subjectivity of effective Pr_{eff} is illustrated, and from Figure 11, it is evident that the flow velocity falls for ascending values Pr_{eff}. A larger value of Pr_{eff} refers to the more momentum diffusivity in the flow domain, which slows down the velocity of the fluid. Figure 12 is sketched to observe the potentness of magnetic parameter M. The pattern of Figure 12 reveals the decreasing trend for the elevating value of M. The effects of a magnetic field in the flow creates some resistive force that opposes the fluid flow that is why fluid velocity decreases for the increasing values of a magnetic parameter.

As it is stated, our prime motive was to make advancements in the research work done by Fetecau et al. [25] for a bigger class of fluid, namely Maxwell fluid. Moreover, it also includes an additional aspect of fractional instead of ordinary derivative. Therefore, the obtained result for velocity is also compared with the result of velocity obtained in [25] graphically. For this purpose, the velocity profiles are sketched in Figure 13 by letting the Maxwell parameter $\lambda = 0$ and fractional parameter $\alpha = 1$ for both slip and nonslip. The overlapping graphic profiles show the validation of our obtained result for velocity.

7. Conclusions

Thermodiffusion is a physical phenomenon that occurs because of the higher temperature and slanting distribution of the mixture. Thermodiffusion results in the isotope separation. In the present study, analytical results for mass and heat transfer flow of Maxwell fluid over a flat plate are considered by taking the effect of the first order slip at the boundary with the fractional derivative, which is known as the CPC fractional derivative. The impacts of radiation and generation of heat are also taken into consideration, along with the effect of a magnetic field of constant magnitude. The pearlized results for velocity, concentration, and temperature are obtained. The graphical illustrations are done using the same graphics of velocity for both cases, slip and no-slip effects. Moreover, this research work may extend to more complex fluids like Oldroyd-B fluid. The conclusions given below are drawn for the present research study.

(1) The fluid flows with an increasing velocity for the variation of α, β, γ, and Sr.

(2) Velocity for Sc, and slip parameter γ_1 is a decreasing function.

(3) For positive N velocity exhibits an enhancing posture the decerned trend for a negative value of N.

(4) For positive Q fluid speeds up, and the negative fluid flow slows down.

(5) The application of the CPC fractional derivative is a far better choice to obtain the generalized solution of the velocity field.

(6) The advantage of the fractional model is nonlocality and flexibility, which is why one can fit the data according to desired results by the variation of the order of fractional derivatives.

Nomenclature

u:	Velocity component along x-axis
t:	Time
ρ:	Density of the fluid
μ:	Viscosity of the fluid
g:	Gravity
β_T, β_C:	Coefficients of volumetric expansion
B_0:	Magnitude of the magnetic field
λ_1:	Maxwell fluid parameter
σ_1:	Stefan–Boltzmann
k:	Thermal conductivity
M:	Magnetic parameter,
Sc:	Schmidt number,
Sr:	Soret effect parameter
Q:	Nondimensional heat generation parameter
${}^{\mathrm{CPC}}D_t^{\alpha}$:	Constant proportional Caputo fractional derivative (CPC)
q_r:	Radiation flux
Q_0:	Heat generation
c_P:	Specific heat at constant pressure
D_m:	Molecular diffusivity,
C_w:	Concentration near the wall.
γ_1:	Slip parameter
C:	Concentration
q:	Laplace transform variable
T_w:	Wall temperature
T_∞:	Ambient temperature
N_r:	Radiation parameter
α, β, γ:	Fractional parameter
N:	Ratio of mass Grashof number to thermal Grashof number
Pr, Pr_{eff}:	Prandtl number and effective Prandtl number
σ:	Current density.

Data Availability

The data used to support the findings of this study are available from the corresponding author upon request.

Conflicts of Interest

The authors declare that there are no conflicts of interest regarding the publication of this paper.

References

[1] A. J. Chamkha and A. Ben-Nakhi, "MHD mixed convection–radiation interaction along a permeable surface immersed in a porous medium in the presence of Soret and Dufour's Effects," *Heat and Mass Transfer*, vol. 44, pp. 845–856, 2008.

[2] O. D. Makinde, "On MHD mixed convection with Soret and Dufour effects past a vertical plate embedded in a porous medium," *Latin American Applied Research*, vol. 41, pp. 63–68, 2011.

[3] D. Vieru, M. A. Imran, and A. Rauf, "Slip effect on free convection flow of second grade fluids with ramped wall temperature," *Heat Transfer Research*, vol. 46, no. 8, pp. 713–724, 2015.

[4] M. Tahir, M. A. Imran, N. Raza, M. Abdullah, and M. Aleem, "Wall slip and non-integer order derivative effects on the heat transfer flow of Maxwell fluid over an oscillating vertical plate with new definition of fractional Caputo–Fabrizio derivatives," *Results in Physics*, vol. 7, no. 3, pp. 1887–1898, 2017.

[5] M. Jamil and N. A. Khan, "Slip effects on fractional viscoelastic fluids," *International Journal of Differential Equations*, vol. 2011, Article ID 193813, 19 pages, 2011.

[6] T. Hayat, M. F. Afzaal, C. Fetecau, and A. A. Hendi, "Slip effects on the oscillatory flow in a porous medium," *Journal of Porous Media*, vol. 14, no. 6, pp. 481–493, 2011.

[7] M. A. Imran, N. A. Shah, K. Rafique, A. Sohail, and S. Ejaz, "General solutions of convective flows of MHD Casson fluid with slip and Radiative heat transfer at the boundary," *Computational Thermal Sciences*, vol. 9, no. 1, pp. 1–11, 2011.

[8] M. Sajid, Z. Abbas, N. Ali, T. Javaid, and I. Ahmad, "Slip flow of a Maxwell fluid past a stretching sheet," *Walailak Journal of Science and Technology*, vol. 11, no. 12, pp. 1093–1103, 2014.

[9] T. Hayat, R. Sajjad, Z. Abbas, M. Sajid, and A. A. Hendi, "Radiation effects on MHD flow of Maxwell fluid in a channel with porous medium," *International Journal of Heat and Mass Transfer*, vol. 54, no. 4, pp. 854–862, 2011.

[10] G. K. Ramesh, B. J. Gireesha, T. Hayat, and A. Alsaedi, "MHD flow of Maxwell fluid over a stretching sheet in the presence of nanoparticles, thermal radiation and chemical reaction: a numerical study," *Journal of Nanofluids*, vol. 4, no. 1, pp. 100–107, 2015.

[11] I. Khan, N. A. Shah, and L. C. C. Dennis, "A scientific report on heat transfer analysis in mixed convection flow of Maxwell fluid over an oscillating vertical plate," *Scientific Report*, vol. 8, Article ID 46975, 2018.

[12] S. Chen, L. Zheng, B. Shen, and X. Chen, "Time–space dependent fractional boundary layer flow of Maxwell fluid over an unsteady stretching surface," *Theoretical and Applied Mechanics Letters*, vol. 5, no. 6, pp. 262–266, 2015.

[13] M. A. Imran, S. Sarwar, M. Imran, and M. Aleem, "Combined effect of slip and radiation on MHD flow past a constantly moving vertical plate with variable temperature," *Journal of Prime Research in Mathematics*, vol. 12, pp. 130–144, 2016.

[14] A. A. Opanuga, H. I. Okagbue, O. O. Agboola, and S. A. Bishop, "Second law analysis of ion slip effect on MHD couple stress fluid," *International Journal of Mechanics*, vol. 12, pp. 96–101, 2018.

[15] T. Hayat and Z. Asghar, "Heat transfer analysis on the peristaltic motion with slip effects," *Zeitschrift für Naturforschung A*, vol. 65, no. 8-9, pp. 697–704, 2010.

[16] T. Hayat, S. Hina, and A. A. Hendi, "Slip effects on peristaltic transport of a Maxwell fluid with heat and mass transfer," *Journal of Mechanics in Medicine and Biology*, vol. 12, no. 1, Article ID 1250001, 2012.

[17] T. Hayat, M. Imtiaz, and A. Alsaedi, "Partial slip effects in flow over nonlinear stretching surface," *Applied Mathematics and Mechanics*, vol. 36, pp. 1513–1526, 2015.

[18] A. Shakeel, S. Ahmad, H. Khan, N. A. Shah, and S. Haq, "Flows with slip of Oldroyd-B fluids over a moving plate," *Advances in Mathematical Physics*, vol. 2016, Article ID 8619634, 9 pages, 2016.

[19] N. A. Shah, C. Fetecau, and D. Vieru, "First general solutions for unsteady unidirectional motions of rate type fluids in cylindrical domains," *Alexandria Engineering Journal*, vol. 57, no. 3, pp. 1185–1196, 2018.

[20] R. A. Shah, T. Abbas, M. Idrees, and M. Ullah, "MHD Carreau fluid slip flow over a porous stretching sheet with viscous dissipation and variable thermal conductivity," *Boundary Value Problems*, vol. 2017, Article ID 94, 2017.

[21] N. Freidoonimehr and S. S. Jafari, "Second law of thermodynamics analysis of hydro-magnetic nano-fluid slip flow over a stretching permeable surface," *Journal of the Brazilian Society of Mechanical Sciences and Engineering*, vol. 37, pp. 1245–1256, 2015.

[22] S. Schneider, "Wall slip effects measuring the rheological behavior of electrorheological (ER) suspensions," *International Journal of Modern Physics B*, vol. 26, no. 1, Article ID 1250006, 2012.

[23] J. Raza, "Thermal radiation and slip effects on magnetohydrodynamic (MHD) stagnation point flow of Casson fluid over a convective stretching sheet," *Propulsion and Power Research*, vol. 8, no. 2, pp. 138–146, 2019.

[24] M. Norouzi, M. Davoodi, O. Anwar Bég, and M. D. Shamshuddin, "Theoretical study of Oldroyd-B visco-elastic fluid flow through curved pipes with slip effects in polymer flow processing," *International Journal of Applied and Computational Mathematics*, vol. 4, Article ID 108, 2018.

[25] C. Fetecau, D. Vieru, C. Fetecau, and I. Pop, "Slip effects on the unsteady radiative MHD free convection flow over a moving plate with mass diffusion and heat source," *The European Physical Journal Plus*, vol. 130, Article ID 6, 2015.

[26] S. A. Khan, Y. Nie, and B. Ali, "Multiple slip effects on MHD unsteady viscoelastic nano-fluid flow over a permeable stretching sheet with radiation using the finite element method," *SN Applied Sciences*, vol. 2, Article ID 66, 2020.

[27] I. Khan, N. A. Shah, Y. Mahsud, and D. Vieru, "Heat transfer analysis in a Maxwell fluid over an oscillating vertical plate using fractional Caputo–Fabrizio derivatives," *The European Physical Journal Plus*, vol. 132, Article ID 194, 2017.

[28] Y.-M. Chu, M. Ijaz Khan, T. Abbas et al., "Radiative thermal analysis for four types of hybrid nanoparticles subject to non-uniform heat source: keller box numerical approach," *Case Studies in Thermal Engineering*, vol. 40, Article ID 102474, 2022.

[29] A. M. Alqahtani, M. Riaz Khan, N. Akkurt, V. Puneeth, A. Alhowaity, and H. Hamam, "Thermal analysis of a radiative nanofluid over a stretching/shrinking cylinder with viscous dissipation," *Chemical Physics Letters*, vol. 808, Article ID 140133, 2022.

[30] V. Puneeth, F. Ali, M. R. Khan, M. S. Anwar, and N. A. Ahammad, "Theoretical analysis of the thermal characteristics of Ree–Eyring nanofluid flowing past a stretching sheet due to bioconvection," *Biomass Conversion and Biorefinery*, 2022.

[31] K. A. M. Alharbi, M. R. Khan, M. Ould Sidi, A. M. Algelany, S. Elattar, and N. A. Ahammad, "Investigation of hydromagnetic bioconvection flow of Oldroyd-B nanofluid past a porous stretching surface," *Biomass Conversion and Biorefinery*, vol. 13, pp. 4331–4342, 2023.

[32] M. R. Khan, S. Algarni, T. Alqahtani, S. A. M. Alsallami, T. Saeed, and A. M. Galal, "Numerical analysis of a time-dependent aligned MHD boundary layer flow of a hybrid nanofluid over a porous radiated stretching/shrinking surface," *Waves in Random and Complex Media*, 2022.

[33] D. Qaiser, Z. Zheng, M. Riaz Khan, and A. M. Galal, "Significance of activation energy and entropy optimization in radiative stagnation point flow of nanofluid with cross-diffusion and viscous dissipation," *Waves in Random and Complex Media*, 2022.

[34] V. Puneeth, M. Shoaib Anwar, and M. Riaz Khan, "Bioconvective Darcy–Frochherimer flow of the Ree–Eyring nanofluid through a

stretching sheet with velocity and thermal slips," *Waves in Random and Complex Media*, pp. 1–14, 2022.

[35] M. R. Khan, A. M. Alqahtani, S. E. Alhazmi et al., "Numerical investigation of Darcy–Forchheimer hybrid nanofluid flow with energy transfer over a spinning fluctuating disk under the influence of chemical reaction and heat source," *Micromachines*, vol. 14, no. 1, Article ID 48, 2023.

[36] L. Kolsi, A. Raza, K. Al-Khaled, K. Ghachem, S. U. Khan, and A. U. Haq, "Thermal applications of copper oxide, silver, and titanium dioxide nanoparticles via fractional derivative approach," *Waves in Random and Complex Media*, vol. 33, no. 3, pp. 794–807, 2023.

[37] Z. Jie, M. Ijaz Khan, K. Al-Khaled et al., "Thermal transport model for Brinkman type nanofluid containing carbon nanotubes with sinusoidal oscillations conditions: a fractional derivative concept," *Waves in Random and Complex Media*, 2022.

[38] A. Raza, S. Ullah Khan, K. Al-Khaled et al., "A fractional model for the kerosene oil and water-based Casson nanofluid with inclined magnetic force," *Chemical Physics Letters*, vol. 787, Article ID 139277, 2022.

[39] A. Raza, A. Ghaffari, S. U. Khan, A. U. Haq, M. I. Khan, and M. R. Khan, "Non-singular fractional computations for the radiative heat and mass transfer phenomenon subject to mixed convection and slip boundary effects," *Chaos, Solitons & Fractals*, vol. 155, Article ID 111708, 2022.

[40] S. U. Khan, S. A. Shehzad, N. Ali, and M. N. Bashir, "Some generalized results for Maxwell fluid flow over porous oscillatory surface with modified Fourier and Fick's theories," *Journal of the Brazilian Society of Mechanical Sciences and Engineering*, vol. 40, Article ID 474, 2018.

[41] S. U. Khan, N. Ali, M. Sajid, and T. Hayat, "Heat transfer characteristics in oscillatory hydromagnetic channel flow of Maxwell fluid using Cattaneo–Christov model," *Proceedings of the National Academy of Sciences, India Section A: Physical Sciences*, vol. 89, pp. 377–385, 2019.

[42] R. Tang, S. Rehman, A. Farooq et al., "Comparative study of natural convection flow of fractional Maxwell fluid with uniform heat flux and radiation," *Complexity*, vol. 2021, Article ID 9401655, 16 pages, 2021.

[43] M. Mansoor, Y. Nawaz, B. Ahmad, and M. Irfan, "Chemically reactive flow and energy transport phenomenon considering variable conductivity on Maxwell fluid: a numerical simulation," *Mathematical Problems in Engineering*, vol. 2022, Article ID 8461613, 9 pages, 2022.

[44] M. A. Imran, M. Aleem, M. B. Riaz, R. Ali, and I. Khan, "A comprehensive report on the convective flow of fractional (ABC) and (CF) MHD viscous fluid subject to generalized boundary conditions," *Chaos, Solitons & Fractals*, vol. 118, pp. 274–289, 2019.

[45] D. Baleanu and A. Fernandez, "On fractional operators and their classifications," *Mathematics*, vol. 7, no. 9, Article ID 830, 2019.

[46] F. Jarad, T. Abdeljawad, S. Rashid, and Z. Hammouch, "More properties of the proportional fractional integrals and derivatives of a function with respect to another function," *Advances in Difference Equations*, vol. 2020, Article ID 303, 2020.

[47] M. Ahmad, M. A. Imran, M. Aleem, and I. Khan, "A comparative study and analysis of natural convection flow of MHD non-Newtonian fluid in the presence of heat source and first-order chemical reaction," *Journal of Thermal Analysis and Calorimetry*, vol. 137, pp. 1783–1796, 2019.

[48] D. Baleanu, A. Fernandez, and A. Akgül, "On a fractional operator combining proportional and classical differ integrals," *Mathematics*, vol. 8, no. 3, Article ID 360, 2020.

[49] J. R. Howell and R. Siegel, *Thermal Radiation Heat Transfer*, Taylor & Francis, New York, 5th edition edition, 2011.

[50] E. Magyari and A. Pantokratoras, "Note on the effect of thermal radiation in the linearized Rosseland approximation on the heat transfer characteristics of various boundary layer flows," *International Communications in Heat and Mass Transfer*, vol. 38, no. 5, pp. 554–556, 2011.

[51] C. Fetecau, D. Vieru, C. Fetecau, and S. Akhter, "General solutions for magnetohydrodynamic natural convection flow with radiative heat transfer and slip condition over a moving plat," *Zeitschrift für Naturforschung A*, vol. 68, no. 10-11, pp. 659–667, 2013.

[52] M. Narahari and B. K. Dutta, "Effects of thermal radiation and mass diffusion on free convection flow near a vertical plate with Newtonian heating," *Chemical Engineering Communications*, vol. 199, no. 5, pp. 628–643, 2012.

[53] H. Stehfest, "Algorithm 368: numerical inversion of Laplace transforms [D5]," *Communications of the ACM*, vol. 13, no. 1, pp. 47–49, 1970.

[54] D. Y. Tzou, *Macro to Microscale Heat Transfer: The Behavior*, Tylor and Francis, Washington, 1970.